Contribution to harmonic balance calculations of self-sustained periodic oscillations with focus on single-reed instruments

Snorre Farner, Christophe Vergez, Jean Kergomard, Aude Lizée

Contribution to harmonic balance calculations of self-sustained periodic oscillations with focus on single-reed instruments

Snorre Farner,[a] Christophe Vergez, Jean Kergomard, and Aude Lizée
Laboratoire de Mécanique et d'Acoustique, CNRS UPR 7051, 31 chemin Joseph Aiguier, 13402 Marseille Cedex 20, France

The harmonic balance method (HBM) was originally developed for finding periodic solutions of electronical and mechanical systems under a periodic force, but has been adapted to self-sustained musical instruments. Unlike time-domain methods, this frequency-domain method does not capture transients and so is not adapted for sound synthesis. However, its independence of time makes it very useful for studying any periodic solution, whether stable or unstable, without care of particular initial conditions in time. A computer program for solving general problems involving nonlinearly coupled exciter and resonator, HARMBAL, has been developed based on the HBM. The method as well as convergence improvements and continuation facilities are thoroughly presented and discussed in the present paper. Applications of the method are demonstrated, especially on problems with severe difficulties of convergence: the Helmholtz motion (square signals) of single-reed instruments when no losses are taken into account, the reed being modeled as a simple spring.

I. INTRODUCTION

Since Helmholtz,[1] it has become natural to describe a self-sustained musical instrument as an exciter coupled to a resonator ["self-sustained" is a term indicating oscillation driven by a constant energy input.] More recently, McIntyre *et al.*[2] have highlighted that simple models are able to describe the main functioning of most self-sustained musical instruments. These models rely on few equations whose implementation is not CPU-demanding, mainly because the nonlinearity is spatially localized in an area small compared to the wavelength. This makes them well adapted for real-time computation (including both transient and steady states). These models are particularly popular in the framework of sound synthesis.

On the other hand, calculation in the frequency domain is suitable for determining periodic solutions of the model (the values of the harmonics as well as the playing frequency) for a given set of parameters. Such information can be provided by an iterative method called the harmonic balance method (HBM). Though the name "harmonic balance" seems to date back to 1936,[3] the method was popularized nearly 40 years ago for electrical and mechanical engineering purposes, first for forced vibrations,[4] later for auto-oscillating systems.[5] The modern version was presented rather shortly after by Nakhla and Vlach.[6] In 1978, Schumacher was the first to use the HBM for musical acoustics purposes with a focus on the clarinet.[7] However, in this paper, the playing frequency is not determined by the HBM. This shortcoming is the major improvement brought 11 years later by Gilbert *et al.*[8] who proposed a full study of the clarinet including the playing frequency as an unknown of the problem.

The fact that the HBM can only calculate periodic solutions may seem a drawback. Certainly, transients such as the attack are impossible to calculate, and the periodic result is boring to listen to and does not represent the musicality of the instrument. Therefore, the HBM is definitely not intended for sound synthesis. Nevertheless, self-sustained musical instruments are usually used to generate harmonic sounds, which are periodic by definition. The HBM is thus very useful for investigating the behavior of a physical model of an instrument, depending on its parameter values. This is possible for both stable and unstable solutions, without care of particular initial conditions, which are necessary in the time domain. Moreover, HBM results can be compared to approximate analytical calculations [like the variable truncation method (VTM)],[9] in order to check the validity of the approximate model considered.

The present paper is based on the work of Gilbert *et al.*[8] Our main contributions are an extension of the diversity of equations managed, improved convergence of the method, introduction of basic continuation facilities, and from a practical point of view, faster calculations. In order to test the convergence properties, especially when the number of harmonics increases, we treat a few extreme cases where exact solutions exist in the form of square (or "rectangular" signals) when losses are ignored. The solutions of such simple models of self-sustained instruments are known to be the so-called Helmholtz motion.

Recently, some of us published a paper discussing the different elements of related clarinet models by using the same software. The influence of the shape of the nonlinear function and of several parameters, such as the reed dynamics or the loss parameter, was studied in the context of cy-

[a]Currently at Department of Electronics and Telecommunications, NTNU, O. S. Bragstads pl. 2, 7491 Trondheim, Norway.

lindrical instruments.[10] In contrast, the model used in the present paper is essentially simple, with neither losses nor reed dynamics. This results in square or rectangular signals, corresponding to instruments with cylindrical and stepped-cone bores, respectively.

While the main idea was already described by Gilbert *et al.*,[8] Sec. II details the principle of the HBM, in particular the discretization of the problem, both in time and frequency.

Section III is devoted to the various contributions of the current work, which are applied in a computer program called HARMBAL.[11] The framework is defined to include models with three equations: two linear differential equations, written in the frequency domain, and a nonlinear coupling equation in the time domain (see Sec. III A). As usual in the HBM, this system of three equations is solved iteratively. The solving method chosen (Newton–Raphson, Sec. II B) has been investigated and its convergence has been improved through a backtracking scheme (Secs. III C and III D).

To illustrate the advantages of the HBM and the improvements, a few case studies were performed and are presented in Sec. IV. They are based on a classical model of single-reed instruments which is presented in Sec. IV A. In Secs. IV B and further, simplifications and variations of the model are introduced so that the results could be compared to analytical calculations, both for cylindrical and stepped-cone bores. Finally, the full model is compared to time-domain simulations. This also shows the modularity of HARMBAL. The comparison is achieved through the investigation of bifurcation diagrams as the dimensionless blowing pressure is altered. The derivation of a branch of solution is obtained thanks to basic continuation with an auto-adaptative parameter step.

Finally, various questions are tackled through practical experience from using HARMBAL. Section V discusses multiplicity of solutions and poor robustness in the frequency estimation.

II. NUMERICAL METHOD

A. The harmonic balance method

The harmonic balance method is a numerical method to calculate the steady-state spectrum of periodic solutions of a nonlinear dynamical system. The following provides a detailed and general description of the method for a nonlinearly coupled exciter-resonator system.

Let $X(\omega_k)$, $k=0,\ldots,N_t-1$ be the discrete Fourier transform (DFT) of one period $x(t)$, $0\leqslant t<T$, of a T-periodic solution of a mathematical system to be defined, where $\omega_k=2\pi k/N_t$. $X(\omega_k)$ will have a number of complex components N_t, which depends on the sampling frequency $f_s=1/T_s$ with which we discretize $x(t)$ into $N_t=T/T_s$ equidistant samples. Each (Fourier) component contains the amplitude and the phase of the corresponding harmonic of the signal. Note that the sampling frequency $f_s=N_t f_p$ is automatically adjusted to the current playing frequency f_p so that we always consider one period of the oscillation while keeping N_t constant. Note also that N_t should be sufficiently large to avoid aliasing. Moreover, if N_t is chosen as a power of 2, the fast Fourier transform (FFT) may be used. Assuming that $N_p<N_t/2$ harmonics are sufficient to describe the solution, we define $\mathbf{X}\in\mathbb{R}^{2N_p+2}$ (i.e., a vector of $2N_p+2$ real components) as the first N_p+1 real components (denoted by $\Re$) of $X(\omega_k)$ followed by their imaginary counterparts ($\Im$)

$$\mathbf{X}=[\Re(X(\omega_0)),\ldots,\Re(X(\omega_{N_p})),\ \Im(X(\omega_0)),\ldots,\Im(X(\omega_{N_p}))]. \tag{1}$$

Note that the components X_0 and X_{N_p+1} are the real and imaginary dc components, respectively (and that X_{N_p+1} is always zero). Our mathematical system can thus be defined by the nonlinear function $F:\mathbb{R}^{2N_p+3}\rightarrow\mathbb{R}^{2N_p+2}$

$$\mathbf{X}=\mathbf{F}(\mathbf{X},f_p). \tag{2}$$

Until now, the playing frequency has silently been assumed to be a known quantity. In autonomous systems, however, the frequency is an additional unknown, so that the N_p-harmonic solution sought is defined by $2N_p+3$ unknowns linked through the $2N_p+2$ equations (2). However, it is well known that as $\mathbf{X}$ is a periodic solution of a dynamical system, and $\mathbf{X}'$ deduced from $\mathbf{X}$ by a phase rotation (i.e., a shift in the time domain) is also a solution. Thus, an additional constraint has to be added in order to select a single periodic solution among the infinity of phase-rotated solutions. A common choice (see Ref. 8) is to consider the solution for which the first harmonic is real (i.e., its imaginary part, X_{N_p+2}, is zero). This additional constraint decreases the number of unknowns to $2N_p+2$ for an N_p-harmonic periodic solution. Thus, we get $\mathbf{F}:\mathbb{R}^{2N+2}\rightarrow\mathbb{R}^{2N+2}$, and it is now possible to find periodic solutions, if they exist.

Finally, a simple way of avoiding trivial solutions to Eq. (2) is to look for roots of the function $\mathbf{G}:\mathbb{R}^{2N_p+2}\rightarrow\mathbb{R}^{2N_p+2}$, defined by

$$\mathbf{G}(\mathbf{X},f_p)=\frac{\mathbf{X}-\mathbf{F}(\mathbf{X},f_p)}{X_1}, \tag{3}$$

i.e., $\mathbf{G}(\mathbf{X},f_p)=0$. This equation is usually solved numerically through an iteration process, for instance by the Newton–Raphson method as in our case. How to handle the playing frequency f_p will be discussed in the following section.

B. Iteration by Newton–Raphson

The equation $\mathbf{G}(\mathbf{X},f)=0$, $\mathbf{G}$ being defined by Eq. (3), is nonlinear and usually has no analytical solution (for readability we leave out the index p on the playing frequency until the end of Sec. III). The Newton–Raphson method is a multidimensional extension of the well-known Newton's method, both of which are available in many text books on calculus, e.g., Ref. 12, Sec. 9.6. This is the method used in the program HARMBAL (see Sec. III), although it had to be refined with a backtracking procedure to improve its convergence, as discussed in Sec. III D.

In our $2N_p+2$-dimensional case, we have a vector problem: we search $(\mathbf{X},f)$ for which $\mathbf{G}(\mathbf{X},f)=0$. As highlighted by Gilbert *et al.*,[8] the playing frequency is unknown and must be included in the root-finding process

$$(\mathbf{X}^{i+1},f^{i+1}) = (\mathbf{X}^i,f^i) - (\mathbf{J}_G^i)^{-1}\cdot\mathbf{G}(\mathbf{X}^i,f^i), \tag{4}$$

where $\mathbf{J}_G^i \triangleq \nabla G(\mathbf{X}^i,f^i)$ is the *Jacobian* matrix of $\mathbf{G}$ at $(\mathbf{X}^i,f^i)$. (The symbol $\triangleq$ indicates that the relation is a definition.) Note that all derivatives by X_{N_p+2}, which was chosen to be zero, are ignored. The column N_p+2 in the Jacobian is thus replaced by the derivatives with respect to the playing frequency f. $\mathbf{J}_G^i$ is thus a $(2N_p+2)$-square matrix. This means that line number N_p+2 in Eq. (4) gives the new frequency f instead of X_{N_p+2}. We define the *Newton step* $\Delta\mathbf{X}=\mathbf{X}^{i+1}-\mathbf{X}^i$ (where $\Delta f=f^{i+1}-f^i$ replaces ΔX_{N_p+2}), which follows the local steepest descent direction.

The Jacobian may be found analytically if $\mathbf{G}$ is given analytically, but it is usually sufficient to use the first-order approximation

$$J_{jk} = \frac{\partial G_j}{\partial X_k} \simeq \frac{G_j(\mathbf{X}+\delta\mathbf{X}_k,f) - G_j(\mathbf{X},f)}{\delta X}, \tag{5}$$

except for $k=N_p+2$, in which case we use

$$J_{j,N+2} = \frac{\partial G_j}{\partial f} \simeq \frac{G_j(\mathbf{X},f+\delta f) - G_j(\mathbf{X},f)}{\delta f}. \tag{6}$$

The components of $\delta\mathbf{X}_k$ are zero except for the kth one, which is the tiny perturbation $\delta X=10^{-5}|X_1|$ or $\delta f=10^{-5}f$. The iteration has converged when $|\mathbf{G}^i| \triangleq |\mathbf{G}(\mathbf{X}^i,f^i)| < \varepsilon$. We found $\varepsilon=10^{-5}$ to be a good compromise between computation time and solution accuracy.

III. IMPLEMENTATION AND HARMBAL

A. Equations for self-sustained musical instruments

Though, to the authors' knowledge, the harmonic balance method in the context of musical acoustics with unknown playing frequency has only been applied to study models of clarinet-like instruments, it should be possible to consider many different classes of self-sustained instruments. It is well accepted that sound production by a musical instrument results from the interaction between an exciter and a resonator through a nonlinear coupling. Moreover, in most playing conditions, linear modeling of both the exciter and the resonator is a good approximation.

Therefore, within these hypotheses, any self-sustained musical instrument could be modeled by the following three equations:

$$\begin{cases} Z_e(\omega)X_e(\omega) = X_c(\omega) & \text{(7a)} \\ X_c(\omega) = Z_r(\omega)X_r(\omega) & \text{(7b)} \\ \mathcal{F}[x_c(t),x_e(t),x_r(t)] = 0, & \text{(7c)} \end{cases}$$

where Z_e and Z_r are the input impedances of the exciter and the resonator, respectively, and X_e and X_r are the spectra describing the dynamics of the exciter and the resonator during the steady state (periodicity assumption). X_c is the spectrum of the coupling variable. All these quantities, and thus Eqs. (7a) and (7b), are defined in the Fourier domain. Equation (7c) is written in the time domain, where $\mathcal{F}$ is a nonlinear functional of x_c, x_e, and x_r, which are the inverse Fourier transforms of X_c, X_e, and X_r, respectively. We apply the discretization as described in Sec. II A, implying that Eqs. (7a) and (7b) become vector equations where the impedances must be written as real $(2N_p+2)\times(2N_p+2)$-matrices to accommodate the rules of complex multiplication

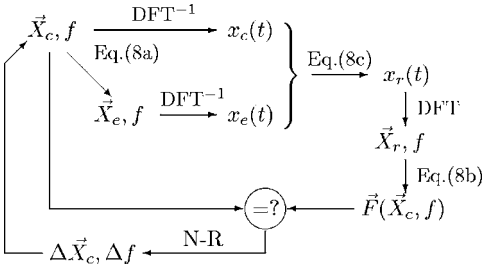

FIG. 1. The iteration loop of the harmonic balance method for a musical instrument (notations defined in the text).

$$Z(f) = \begin{pmatrix} \Re[\tilde{Z}(f)] & -\Im[\tilde{Z}(f)] \\ \Im[\tilde{Z}(f)] & \Re[\tilde{Z}(f)] \end{pmatrix} \tag{8}$$

where

$$\tilde{Z}(f) = \begin{pmatrix} Z(0) & 0 & \cdots & 0 \\ 0 & Z(\omega_1) & & 0 \\ \vdots & & \ddots & \vdots \\ 0 & 0 & \cdots & Z(\omega_{N_p}) \end{pmatrix} \tag{9}$$

is complex, and $\Re(\tilde{Z})$ and $\Im(\tilde{Z})$ are the real and imaginary components of $\tilde{Z}$. The system (7) is solved iteratively by HARMBAL according to the scheme illustrated in Fig. 1.

In HARMBAL, these equations are easily defined by writing small, new C functions. Only superficial knowledge of the C language is necessary to do this.

Three cases related to models of single-reed instruments with cylindrical or stepped-conical bores are studied in particular in Sec. IV in order to validate the code and to illustrate the modularity of HARMBAL and the HBM.

B. Practical characteristics of HARMBAL

Fast calculation, good portability, and independence of commercial software are easily achieved by programming in C, whose compiler is freely available for most computer platforms. It is, however, somewhat difficult to combine portability with easy usage, because an intuitive usage normally means a graphical and interactive user interface, while the handling of graphics varies greatly between the different platforms.

We have chosen to write HARMBAL with a nongraphical and noninteractive user interface. (The term "noninteractive" means that the user has no influence on the program while it is running.) The major advantage of this is that independent user interfaces may be further developed depending on need.

Our concept is to save both the parameters and the solution in a single file. This file also serves as input to HARMBAL while individual parameters can be changed through start-up arguments. The solution provided by the file works as the initial condition for the harmonic balance method. Thus, the lack of a simple user interface is compensated by a simple way of reusing an existing solution to solve the sys-

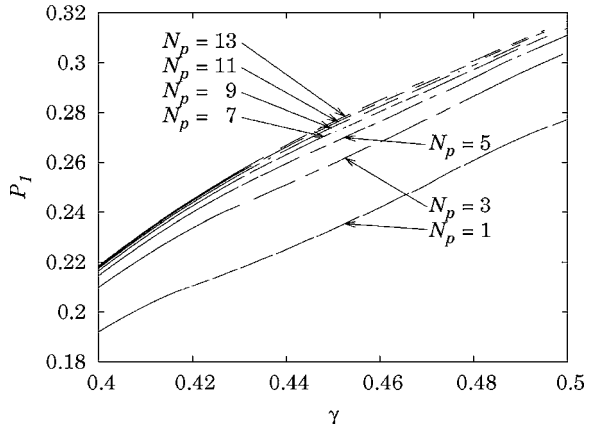

FIG. 2. Solution holes: first pressure harmonic P_1 versus blowing pressure γ for different N_p with N_t=128, ζ=0.5, and η=10^{-3}. (Even N_p give the same as N_p-1.) Equations and parameters are defined in Sec. IV.

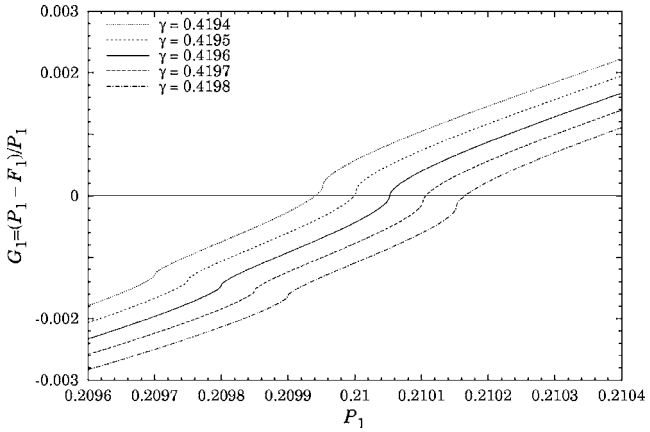

FIG. 3. G_1 as a function of P_1 around the solution G_1=0 for various γ around a hole at $\gamma\simeq$0.4196. N_t=128 and N_p=1.

tem for a slightly different set of parameters. Solutions for a range of a parameter values may thereby be calculated by changing the parameter stepwise and providing the previous solution as an initial condition for the next run. The Perl script *hbmap* provides such zeroth-order continuation facilities. This procedure may also be used when searching for a solution where it is difficult to provide a sufficiently good initial condition, for instance by successively increasing N_p when wanting many harmonics.

C. Convergence of Newton–Raphson

When employing the method in its standard version to determine the solution of the system at a given set of parameters, we have found that it is impossible to find a solution at particular combinations of parameter values. Indeed, for the clarinet model of Sec. IV B 1, no convergence was obtained for particular values of the parameter γ (the dimensionless blowing pressure) and its neighborhood. This is seen as discontinuities, or *holes*, in the curves in Fig. 2 (see Sec. IV for the underlying equations and parameters). Note that the solutions seem to go continuously through this hole and that the positions of the holes and their extent vary with the number of harmonics N_p taken into account. The curves were obtained by using *hbmap* to calculate a quasicontinuity of solutions descending from γ=0.5 in steps of 10^{-4} and drawing a line between them, except across γ values where solution failed. In these holes, the Newton–Raphson method did not converge either by alternating between two values of $\mathbf{P}$ (i.e., $\mathbf{X}_c$) or by starting to diverge.

To study the problem, we simplified the system to a one-dimensional problem by setting N_p=1, thus leaving P_1 as the only nonzero value. G_1 thus became the only contributor to $|\mathbf{G}|$, and a simple graph of G_1 around the solution G_1=0 could illustrate the problem, as shown in Fig. 3 for several values of γ. We see that the curve of $G_1(P_1)$ has inflection points (visible as "soft steps" on the curve) at rather regular distances. At the center of a convergence hole, in this case at γ=0.4196, an inflection point is located at the intersection with the horizontal axis. This is a school example of a situation where Newton's method (the one-dimensional limit of the Newton–Raphson method) does not converge because the Newton step ΔP_1 brings us alternatingly from one side of the solution to the other, but not closer.

In fact, the existence of inflection points is linked with the digital sampling of the continuous signal. If the sampling rate is increased, i.e., if N_t is increased, the steps become smaller but occur more frequently, as shown for N_t=32, 128, and 1024 in Figs. 4(a)–4(c). The derivative dG_1/dP_1 is included in the figures to quantify the importance of the steps. According to Figs. 4(a)–4(c), it seems reasonable to increase N_t to avoid convergence problems. However, this would significantly increase the computational cost. Another solution is therefore suggested in the following.

D. Backtracking

When the Newton–Raphson scheme fails to converge, it often happens because the Newton step $\Delta\mathbf{X}$ leads to a point

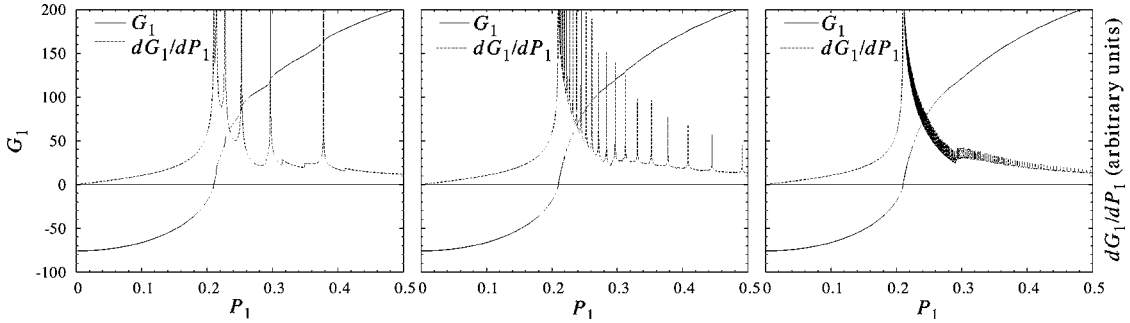

FIG. 4. The effect of sampling rate on the "smoothness" of $G_1(P_1)$: (a) N_t=32; (b) 128; and (c) 1024. The derivative dG_1/dP_1 exhibits the "roughness."

TABLE I. Description of variables and constants. The dimensionless variables and parameters used in Sec. IV are derived from dimensional variables [denoted by a hat (∧)] as follows: $x_e = x = \hat{y}/H + \gamma/K$, $x_c = p = \hat{p}/p_M$, $x_r = u = \hat{u}\rho c/Sp_M$, $\omega = \hat{\omega}/f_r$, $\gamma = p_m/p_M$, and $\zeta = (Hw/S)\sqrt{2\rho c^2/p_M}$. The dimensionless time is $t = \hat{t}\omega_r$. The coefficients of the reed equation are $M = K\omega_r^2/\omega_e^2$, $R = Kg_e\omega_r/\omega_e^2$, and $K = \mu_e H\omega_e^2/p_M$. Note that index e denotes exciter and r resonator. SI units in parentheses.

$\hat{y}$	displacement of reed from equilibrium (m)
$\hat{p}$	pressure in reed opening (Pa)
$\hat{u}$	volume flow though reed opening (m^3/s)
$\hat{f}_r$	first mode frequency of pipe (Hz)
f_p	playing frequency (Hz)
p_m	mouth pressure/blowing pressure (Pa)
p_M	pressure p_m that closes reed opening (Pa)
H	equilibrium height of reed opening (m)
w	width of reed opening (m)
S	cross section of the pipe (m)
g_e	damping of the reed (s^{-1})
μ_e	specific mass of the reed (kg/m^2)
ω_e	first mode angular frequency of the reed (s^{-1})
ω_r	first mode angular frequency of the pipe ($2\pi f_r$; s^{-1})
Z_c	characteristic input impedance of the pipe ($\rho c/S$)
η	dimensionless loss parameter for the pipe
ρ	density of air (kg/m^3)
c	sound speed in air (m/s)

where $|\mathbf{G}(\mathbf{X},f)|$ is larger than in the previous step. However, acknowledging that the Newton step points in the direction of the steepest descent, there must be a point along $\Delta\mathbf{X}$ where $|\mathbf{G}(\mathbf{X},f)|$ is smaller than in the previous iteration of the HBM. A backtracking algorithm described in Sec. 9.7 of Ref. 12 (see the Appendix) solves the problem elegantly by shortening the Newton step to $\lambda\Delta\mathbf{X}$ for $0<\lambda<1$.

IV. CASE STUDIES

A. Equations for the clarinet

The three equations (7a)–(7c) may be constructed by physical modeling. In the case of the clarinet, a common simple model can be constructed by a reed equation nonlinearly coupled to a pipe equation by the Bernoulli equation.[7,10,13–15] The equations are summarized below in dimensionless form with the variables and constants defined in Table I. The corresponding mouthpiece is illustrated in Fig. 5.

The exciter is an oscillating reed which may be modeled as a spring with mass and damping

$$M\ddot{x} + R\dot{x} + Kx = p, \tag{10}$$

where the dimensionless reed displacement x (dots denoting time derivative) is the exciter variable x_e and the pressure p in the mouthpiece is the coupling variable x_c. The coefficients $M = \omega_r^2/\omega_e^2$, $R = g_e\omega_r/\omega_e^2$, and $K = 1$ are the dimensionless mass, damping, and spring constant of the reed, where g_e is the reed damping and ω_r and ω_e are the first mode angular frequencies of the resonator and the exciter, respectively. $K = 1$ because the reed closes when blowing at the maximum blowing pressure in the static regime ($p = 0$). The exciter impedance in Eq. (7a) thus becomes

$$Z_e(\omega) = K - M\left(\frac{\omega}{2\pi}\right)^2 + iR\left(\frac{\omega}{2\pi}\right), \tag{11}$$

where the dimensionless angular frequency ω is 2π at the first resonance of the pipe.

The cylindrical quarter-wave resonator is simply described by the dimensionless input impedance to be used in Eq. (7b)

$$Z_r(\omega) = i\tan\left(\frac{\omega}{4} - i\alpha(\omega)\right), \tag{12}$$

where $\alpha(\omega) \triangleq \psi\eta\sqrt{\omega/2\pi}$ is the dissipation in the tube, $\psi \simeq 1.3$, and η being the dimensionless loss parameter. Here, η depends on the tube length and is typically 0.02 for a normal clarinet with all holes closed. We set η to almost zero in our lossless calculations.

Finally, the nonlinear coupling equation (7c) is given by relating the volume flow u of air through the reed opening, i.e., the coupling variable x_c, to x and p by the Bernoulli equation. Taking into account high blowing pressures γ, the dimensionless version becomes[14]

$$u(p,x) = \zeta(1 + x - \gamma)\sqrt{|\gamma - p|}\,\mathrm{sign}(\gamma - p), \tag{13}$$

as long as $x > \gamma - 1$, and $u = 0$ otherwise because the reed closes the mouthpiece, i.e., the reed "beats." ζ is a dimensionless embouchure parameter roughly describing the mouthpiece and the position of the player's lips. Only the nonbeating-reed regime is considered in this study.

Disregarding the reed dynamics, i.e., considering the reed mass and damping negligible, we have $x = p$ instead of Eq. (10). The exciter impedance thus simplifies to $Z_e = 1$ and the coupling equation to

$$u(p) = \zeta(1 + p - \gamma)\sqrt{|\gamma - p|}\,\mathrm{sign}(\gamma - p) \tag{14}$$

for $p > \gamma - 1$, and, as before, $u = 0$ otherwise.

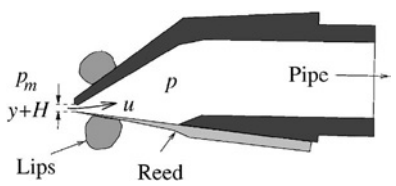

FIG. 5. Illustration of the mouthpiece. The mouth pressure p_m becomes γ in dimensionless quantities, and the instantaneous reed opening $y+H$ becomes $x_e - \gamma + 1$ (see Table I).

B. Verification of method and models

In the following we want to verify that the HBM (and its implementation in HARMBAL) gives correct results. By using very low losses in the resonator (small η) and disregarding the reed dynamics, we can compare the results of the HBM with analytical results. Moreover, we can compare our results with numerical results from real-time synthesis. For this we need to include mass and damping of the exciter. These case studies also illustrate the modularity of HARMBAL as both the exciter and the resonator are changed. An example of changing the coupling equation is shown by Fritz *et al.*[10]

1. Helmholtz oscillation for cylindrical tubes

To compare the HBM results with analytical results, we assume a nondissipative air column, i.e., setting $\eta = 0$ and

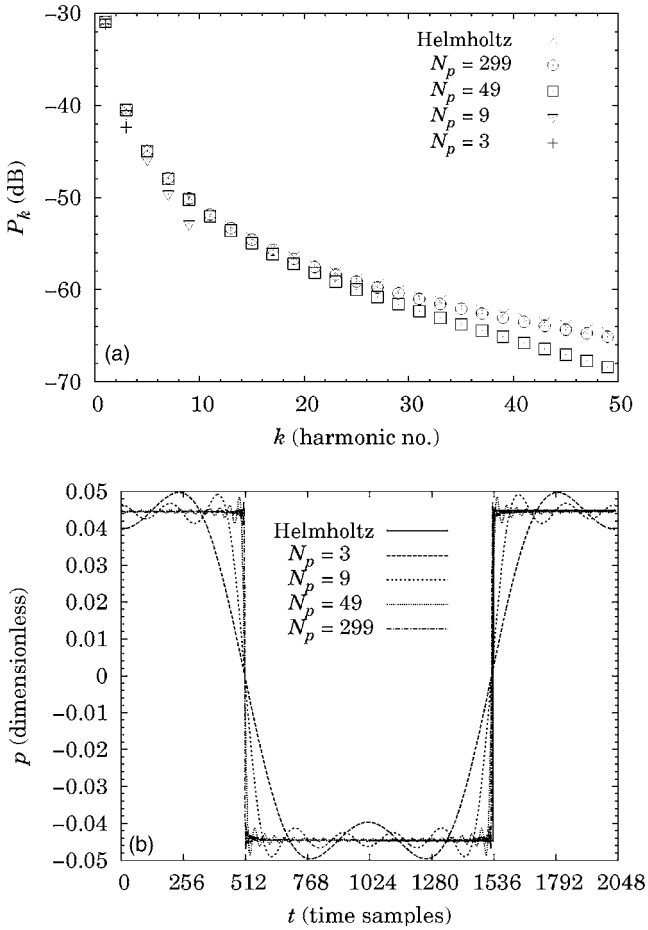

FIG. 6. The Helmholtz solution, Eq. (15), compared with the HBM truncated to 3, 9, 49, and 299 harmonics close to the oscillation threshold (γ =0.334, ζ=0.5, η=10^{-5}) in (a) frequency and (b) time domain.

thus α=0 in Eq. (12). Furthermore, we neglect reed dynamics and thus use Z_e=1 and Eq. (14). The resulting square-wave amplitude (the Helmholtz motion)[1] may be found by solving $u(p)$=$u(-p)$, which results from the fact that the internal pressure $p(t)$ and the power $p(t)u(t)$ averaged over a period are zero according to the lossless hypothesis.[14] This leads to a square-wave oscillation with amplitude

$$p(\gamma) = \sqrt{-3\gamma^2 + 4\gamma - 1}. \tag{15}$$

As shown in Fig. 6, the HBM solution close to the oscillation threshold shows very good convergence towards the Helmholtz motion as the number of harmonics increases. Note that the points do not match for higher harmonics, not even for 299 harmonics. Dissipation in the resonator ($\eta \neq 0$) causes higher harmonics to be damped more close to the threshold ($\gamma \simeq 1/3$) than for higher blowing pressures (as explained, e.g., in Ref. 9). The deviation from a square-wave signal is thus more noticeable close to the threshold, and as the HBM calculations imposed a nonzero dissipation, this is probably the reason for the small deviation in Fig. 6. Our calculations at γ=0.4 confirm that the HBM results for N_p=299 approach the Helmholtz motion further away from the threshold.

Figure 2 in Ref. 10 shows P_1 as a function of γ for various N_p for η=0.02, calculated by HARMBAL. A similar diagram may be made for the lossless case here, as shown in

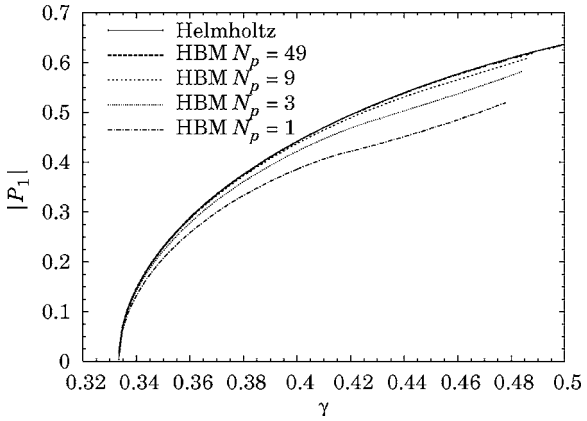

FIG. 7. Amplitude of first harmonic as the blowing pressure increases for the Helmholtz solution (15) and the HBM truncated to N_p harmonics (ζ =0.5, η=10^{-5})

Fig. 7. The oscillation threshold is reduced to γ=1/3, at which point the model experiences a direct Hopf bifurcation (which is known since the work of Grand *et al.*),[16] i.e., the oscillation starts continuously from zero as γ is increased beyond the threshold. This means that a single harmonic is enough to study the solution around the threshold. Far from the threshold, more harmonics have to be taken into account for P_1 to converge toward the Helmholtz solution. This is not obvious and contradictory to the hypothesis made for the VTM,[9] for example. Thus, HARMBAL appears as an interesting tool to evaluate the relevance of approximate methods at certain parameter values.

2. Helmholtz oscillation for a stepped conical tube

The saxophone works similarly to the clarinet, but the bore has a conical shape. In this section we compare HBM calculations with analytical results, so we simplify the cone by assuming that it consists of a sequence of N cylinders of length l and cross section S_i=$\frac{1}{2}i(i+1)S_1$ for i=1,…,N and S_1=S being the cross section of the smallest cylinder (see Ref. 17). The total length of the instrument is thus L=Nl. The input impedance of such a *stepped cone* may be written as

$$Z_r(\omega) = \frac{2i}{\cot(\omega'/4 - i\alpha(\omega')) + \cot(\omega' N/4 - i\alpha(\omega' N))}, \tag{16}$$

where $\omega' \triangleq 2\omega/(N+1)$ so that ω=2π at the first resonance of this resonator. Equation (16) is used instead of Eq. (12), and the losses $\alpha(\omega)$ are zero in the analytic Helmholtz case and very small for the HBM calculations (η=$2\cdot10^{-5}$, below which convergence became difficult).

Similarly to the cylinder case, the pressure amplitude of the ideal lossless stepped cone is calculated by solving $u(p)$=$u(-Np)$. Two solutions are possible [This result corrects Eq. (14) in Ref. 17]:

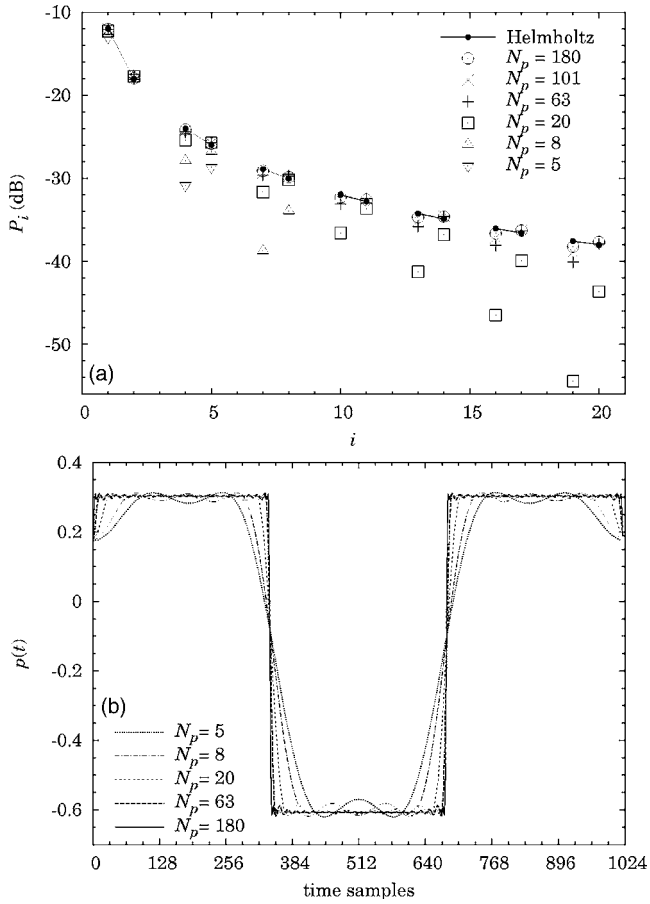

FIG. 8. Comparison between the standard Helmholtz motion of a stepped cone (N=2) and the HBM for various N_p at γ=0.31, ζ=0.2, and η =2·10^{-5}. (a) The magnitude of the harmonics and (b) one oscillation period. N_t varies from 128 for N_p=5 to 1024 for N_p=180.

$$p^{\pm}(\gamma) = \frac{(N-1)(2-3\gamma)}{2(N^2-N+1)} \pm \frac{\sqrt{(N-1)^2+(N+1)^2(-3\gamma^2+4\gamma-1)}}{2(N^2-N+1)}, \qquad (17)$$

as long as $\gamma < 1/(N+1)$ for the standard Helmholtz motion (p^+) and $\gamma < N/(N+1)$ for the inverted one (p^-), which is unstable. Above these limits $p^+=\gamma$ and $p^-=-\gamma/N$. The magnitude of the first harmonic of a square or rectangular wave is then given by

$$P_1^{\pm}(\gamma) = \frac{\sin(\pi/(N+1))}{\pi/(N+1)} p^{\pm}(\gamma). \qquad (18)$$

For N=1, Eq. (17) reduces to Eq. (15). For higher N, the pressure wave becomes asymmetric.

We take the case N=2 and get

$$p^{\pm}(\gamma) = \tfrac{1}{6}(2-3\gamma \pm \sqrt{-27\gamma^2+36\gamma-8}). \qquad (19)$$

This result is compared with HBM calculations in Fig. 8 for γ=0.31. Theoretically, the spectrum of the Helmholtz solution, Fig. 8(a), shows that every third component is missing (actually zero) while the remaining components decrease in magnitude, thus forming the asymmetric pressure oscillation as shown in Fig. 8(b). The HBM, on the other hand, arrives at a solution where the first component

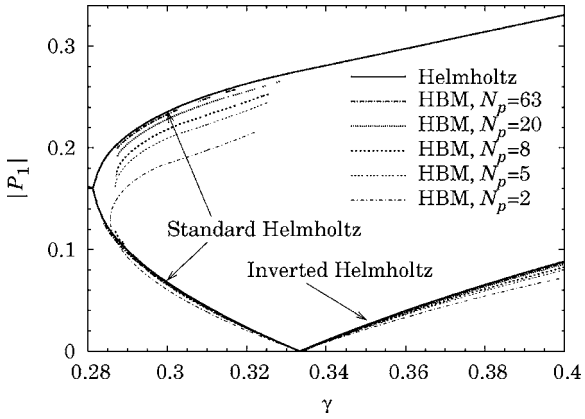

FIG. 9. Amplitude of first harmonic P_1 as a function of the blowing pressure γ for the Helmholtz solution (19) for two-stepped cone and the HBM truncated to 2, 5,…, and 63 harmonics, the last coinciding with Helmholtz (ζ =0.2, η=2·10^{-5}). Only nonbeating regimes are shown.

in each pair of nonmissing components, i.e., components 1, 4, 7, etc., deviate more from the Helmholtz solution than the second component, i.e., 2, 5, 8, etc. This results in a *dip* at the middle of the long, positive part of the period [i.e., on both extreme times 0 and 1024 of the curve in Fig. 8(b)]. The same was observed for N=3 and N=4, where the long part of the period was divided by similar dips into three and four parts, respectively (not shown). The number of time samples, N_t, did not change this fact, but as Fig. 8 indicates, the dips gradually become narrower as the number of harmonics N_p increases. This indicates that the HBM approaches the Helmholtz solution as N_p approaches infinity.

A bifurcation diagram is plotted in Fig. 9, i.e., the amplitude of the first harmonic is plotted for different numbers of harmonics as a function of the blowing pressure γ. This was done by first finding the solution at γ=0.31; then, the script *hbmap* was used to make HARMBAL calculate a solution for each of many consecutive values of γ down to the oscillation threshold by using the previous solution as initial value. The procedure was repeated from the solution at γ =0.31 up to the point where the reed started to beat, i.e., where $p<\gamma-1$ in Eq. (14). In practice, these curves are more difficult to obtain with *hbmap* than for the cylindrical bore, especially close to the subcritical oscillation threshold around γ=0.28, where computation was not possible at these low losses. More sophisticated continuation schemes should be considered to obtain complete curves.

The Helmholtz solution [Eq. (18) with N=2] is included with a solid line in Fig. 9. The lower part of the standard Helmholz branch and the branch of the inverted Helmholtz motion (see the figure) are unstable.[18]

Despite the uncompleted curves, the diagram shows that the model experiences a subcritical Hopf bifurcation, which agrees with the conclusion of Grand *et al.*[16] This means that a single-harmonic approximation is not enough to study the solution around this threshold, since the small-amplitude hypothesis with few harmonics close to the threshold does not hold. Convergence toward the Helmholtz motion is ensured as the number of harmonics N_p is increased. It can be noted that the beating threshold for the model with N_p harmonics

TABLE II. The values of M and R for three strengths of reed interaction. The bore parameters are D=247 (f_r=103.4 Hz), a_1=0.899, and b_0=0.0946 for sampling frequency f_s=51 100 Hz

Reed	$\omega_e/2\pi$ Hz	q_e	M	R
Weak	10 000	0.1	$1.070\cdot10^{-4}$	$1.034\cdot10^{-3}$
Normal	2 500	0.2	$1.712\cdot10^{-3}$	$8.28\cdot10^{-3}$

depends on N_p but converges toward the Helmholtz threshold $\gamma=1/3$ (corresponding to the lossless, continuous system) as N_p is increased.

3. Validation with time-domain model

When adding mass and damping to the reed, and viscous losses or dispersion to the pipe, it becomes more difficult to find analytic solutions to compare with the HBM. As far as the playing frequency is concerned, this has been studied by Fritz *et al.*[10] by comparison with an approximate analytical formula. Here, we compare both the playing frequency and the amplitude of the first partial with numerical results obtained with a time-domain method. We use a newly developed (real-time) time-domain method (here called TDM) by Guillemain *et al.*[19] It is based on the same set of equations as presented in Sec. IV A except that the impedance of the bore is modified a little to be expressed as an infinite impulse response. In the Fourier domain it becomes

$$Z_r(\tilde{\omega}) = \frac{1 - a_1 e^{-i\tilde{\omega}} - b_0 e^{-i\tilde{\omega}D}}{1 - a_1 e^{-i\tilde{\omega}} + b_0 e^{-i\tilde{\omega}D}}, \tag{20}$$

where $\tilde{\omega}$ is the angular frequency normalized by the sampling frequency f_s, and the integer D=round($f_s/2f_r$) is the time delay in samples for the sound wave to propagate to the end of the bore and back. The constants a_1 and b_0 are to be adjusted so that the first two peaks of resonance have the same amplitude as the first two peaks of Eq. (12).

To express Eq. (20) using our terminology, we write that $\omega=\tilde{\omega}f_s/f_r$ and obtain

$$Z_r(\omega) = \frac{1 - a_1 e^{-i\omega f_r/f_s} - b_0 e^{-i\omega/2}}{1 - a_1 e^{-i\omega f_r/f_s} + b_0 e^{-i\omega/2}}. \tag{21}$$

Because the TDM does not work for zero or even for small values of the mass M and damping R, we include reed dynamics in the calculations and use a reed with weak interaction with the pipe resonance as well as one with close to normal reed impedance. The corresponding values for ω_e and $q_e \triangleq g_e/\omega_e$ are shown in Table II. Figure 10(a) shows the bifurcation diagram for two values of ζ and for weak and normal reed impedance, while Fig. 10(b) shows the corresponding variation in the dimensionless playing frequency f_p/f_r. The lines represent the continuous solutions of the HBM, and the symbols show a set of results derived from the steady-state part of the TDM signal. The TDM symbols fall well on the lines of the HBM, except for ζ=0.50 when γ approaches 0.5. Then, the TDM experiences period doubling, i.e., two consecutive periods of the signal differ. At the same time, not being able to show subharmonics, the HBM shows signs of a beating reed, possibly a solution that is unstable and thus not attainable by time-domain methods.

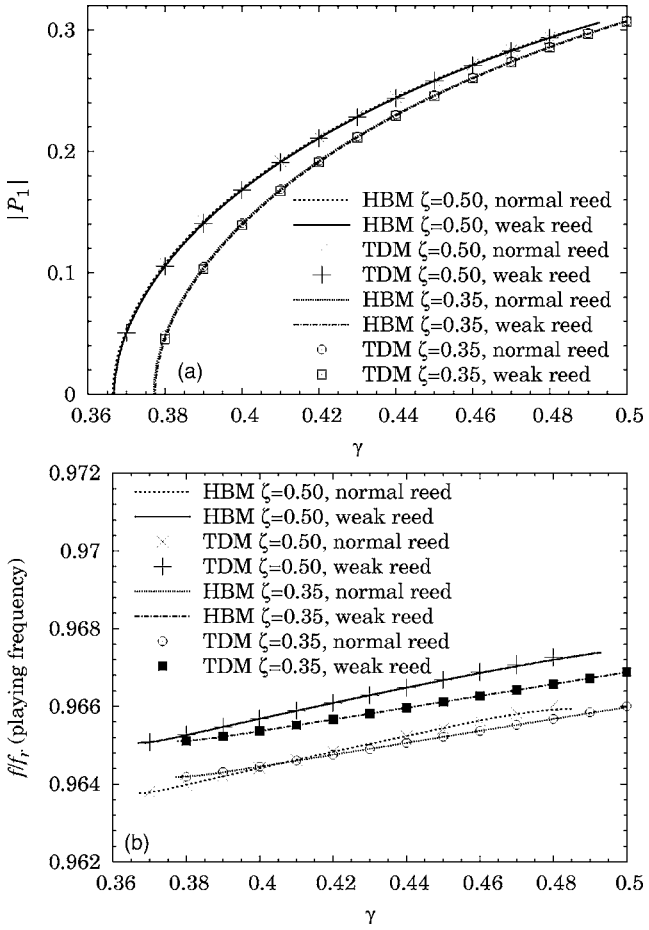

FIG. 10. Comparison between HBM and TDM of the amplitude of (a) the first harmonic P_1 and (b) the dimensionless playing frequency f_p/f_r as the blowing pressure γ increases for a clarinet-like system with viscous losses and weak and normal reed interaction. TDM values for ζ=0.50 and γ >0.48 are omitted due to period doubling, as are the beating regimes of HBM calculations (f_s=51100 Hz, N_t=512, f_r=103.4 Hz, N_p=15).

Note that three points have to be verified before comparing results from the HBM and the TDM:

(1) The numerical scheme used in the TDM to approximate the time derivatives in the reed equation (10) requires discretization. Depending on the sampling frequency f_s, the peak of resonance of the reed deviates more or less from the one given by the continuous equation. For normal reed interaction ($\omega_e/2\pi$=2500 Hz), the deviation is negligible, but it may become significant in the case of weak reed interaction, where the peak is at 10 000 Hz. However, the fact that the reed and the bore interact weakly in the latter case implies that the exact position of the peak has little importance. Therefore, at the used sampling frequency, it was not necessary to compensate for the discretization in the TDM in the HBM calculations.

(2) Then, there should be agreement between the sampling frequency f_s in the TDM and the number of samples N_t per period in the HBM. Their relation is given by

$$N_t = \frac{f_s}{f_p}. \tag{22}$$

In order to have a sufficiently high sampling rate, we

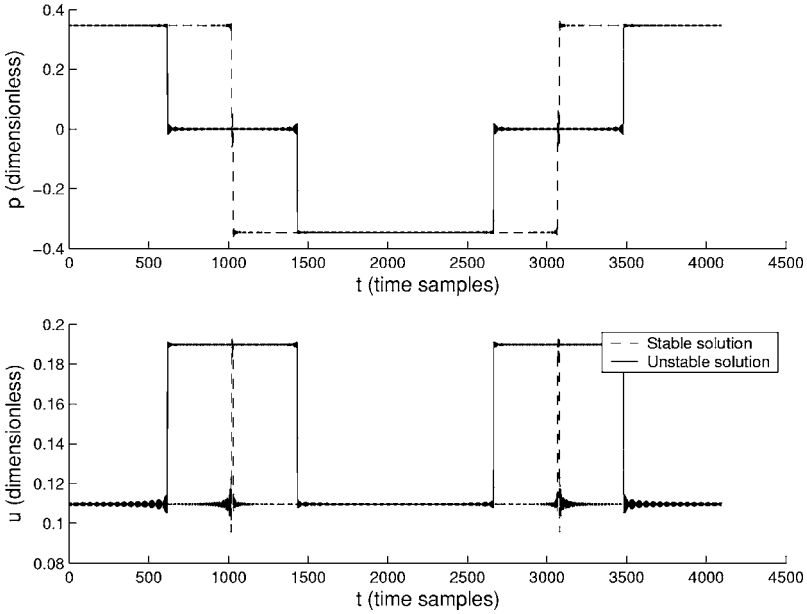

FIG. 11. The pressure and volume-flow wave form of the Helmholtz solution and a three-level sister solution calculated by the HBM employing the simple clarinet model with $\zeta=0.5$, $\gamma=0.4$, $N_p=2000$, $\eta=10^{-5}$.

have chosen $N_t=512$. The playing frequency f_p is plotted in Fig. 10(b), and we used an average $f_s=51\,100$ Hz for both the HBM and the TDM.

(3) Finally, it also seems necessary that N_p and N_t are chosen so that

$$N_p + 1 = \frac{N_t}{2}. \tag{23}$$

In practice, however, when comparing bifurcation diagrams of the first harmonic P_1, as in Fig. 10, rather low values of N_p give good results. Nevertheless, more harmonics are obviously needed to compare waveforms in the time domain, especially far from the oscillation threshold.

V. PRACTICAL EXPERIENCES

A. Multiple solutions

As we consider a nonlinear problem, we cannot anticipate the number of solutions. Therefore, it should not be surprising that it is possible to obtain multiple solutions for a given set of parameter values. When searching for a particular solution, this may be a practical problem. Fritz *et al.*[10] have discovered that some solutions seem to disappear when increasing the number of harmonics N_p, implying that solutions may arise from the truncation to a finite N_p. We have now discovered alternative solutions that persist even at very high N_p.

Let us illustrate this with the simple model of the clarinet used in Sec. IV B 1, where the reed is a spring without mass or damping, the nonlinearity is given by Eq. (14), and the bore is an ideal cylinder with nearly lossless propagation. Figure 11 shows a three-level sister solution together with the related Helmholtz solution for a large number of harmonics, $N_p=2000$.

A solution of the lossless problem should satisfy the criteria (the dimensionless period being 2π) (Ref. 14).

$$\begin{cases} p(t+\pi) = -p(t) \\ u(t+\pi) = u(t), \end{cases} \tag{24}$$

which, for a square signal, is equivalent to the conditions stated before Eq. (15), noting that $p(t)=u(t)=0$ for all t is the static solution. It is easily verified graphically that both of the solutions in Fig. 11 satisfy these conditions. Moreover, since they also satisfy Eq. (14) at any time, the three-level solution is a solution of the lossless model.

Whereas the system of time-domain equations (24) has an infinity of solutions, truncation in the frequency domain limits the number of solutions. The unique solution of the HBM with only one harmonic is obviously a sine. Let us analyze the situation in the simplest nontrivial case of the lossless problem with two odd harmonics and a cubic expansion for nonlinear coupling. Ignoring even harmonics, the HBM gives a system of two equations (see Ref. 9)

$$\begin{cases} \alpha = 3P_1^2(1 + x + 2|x|^2) & \text{(25a)} \\ \alpha x = P_1^2(1 + 3x|x|^2 + 6x), & \text{(25b)} \end{cases}$$

where $\alpha=-A/C$ and $x=P_3/P_1$. As Eq. (25a) imposes P_3 to be real, solving this system amounts to solving

$$x^3 + x^2 - x = 1/3. \tag{26}$$

This equation has three real solutions: $x\simeq -1.5151$, -0.2776, and 0.7926. All of them are found by HARMBAL for negligible losses ($\eta=10^{-5}$), and the corresponding waveforms are presented in Fig. 12. We note that the second solution leads to the Helmholtz motion when increasing the number of harmonics (with the theoretical value known to be $x=-1/3$), whereas the third one corresponds to the three-level solution in Fig. 11. We can also easily imagine that these three solutions of the truncated problem are three-harmonic approximations of square waves that are distributed on three levels: $p^{\pm}\simeq\pm 0.5$ and $p=0$. It should be noted that the conditions (24) for the continuous problem do not constrain the duration of each step. This has to be kept in mind when increasing N_p using the HBM.

While the Helmholtz motion is known to be stable,[14] the two three-level solutions can be considered as a combination of the static solution (the zero level) and the square wave

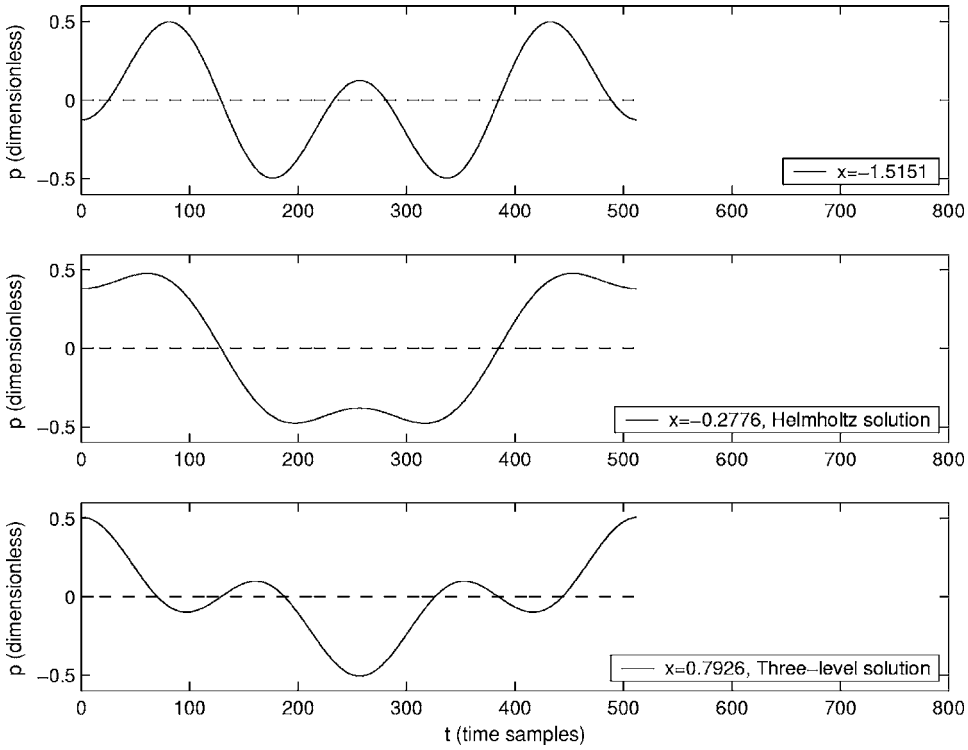

FIG. 12. The pressure waveform of the three solutions found by the HBM with N_p=3 employing the simple clarinet model with ζ=0.5, γ=0.4, η =10^{-5}.

(two levels with opposite values). Since we know from Kergomard[14] that in the case of ideal propagation without losses the stability domains of these two solutions are mutually exclusive, it can be concluded that the three-level solutions are unstable.

Taking into account losses in the propagation does not make the three-level solutions vanish. But, a simple reasoning to determine the stability of this solution is not possible in this case. To the authors' knowledge, however, such a solution has never been observed experimentally at low level of excitation.

B. Initial value of the playing frequency

A practical difficulty encountered is the convergence of the playing frequency f_p. If its initial value is not close enough to the solution, divergence is almost inevitable. This occurs because the resonator impedance Z_r tends to vanish outside the immediate surroundings of the resonance peaks of the resonator, rendering $\mathbf{F}(\mathbf{P},f_p)$ very small and thereby $\mathbf{G}\simeq\mathbf{P}/P_1$ nearly constant with respect to f_p. The slope $\partial\mathbf{G}/\partial f_p$ thus becomes close to zero, the Newton step leads far away from the solution, and convergence fails. Dissipation widens the resonance peaks and thus also the convergence range.

For a simple system where the playing frequency is known to correspond to a resonance peak of the tube, initializing f_p is easy. However, with dispersion or other inharmonic effects, choosing an initial value for f_p may be difficult. In HARMBAL the problem may to some extent be avoided by the possibility of gradually adding the dispersion (or other inharmonic effects), so that the playing frequency can be followed quasicontinuously from a known solution without dispersion, for instance by using *hbmap*.

VI. CONCLUSIONS

The harmonic balance method (HBM) is suited for studies of self-sustained oscillations of musical instruments, and the computer program HARMBAL has been developed for this application. It is available with its source code,[11] has a free license, and is already in use by several researchers. It is programed in C, runs fast, and is easily used by other applications, such as for continuation purposes.

Some difficulties are related to the digital sampling of the signal and can be solved by introducing a backtracking mechanism. When using a large number of harmonics, the extreme case of the (lossless) Helmholtz motion can be solved for different shapes of resonators. Nevertheless, the value of the first harmonic P_1 seems to be well predicted by lower values of N_p, in particular close to the threshold of a direct bifurcation. For the saxophone we used a stepped-cone bore and observed one or more dips during the longest part of the period, depending on the number of steps. These dips approach pure impulses as N_p increases. The number of samples N_t in a period proved to be insignificant for these dips.

The HBM can lead to some alternative solutions for a unique set of parameters. The nondissipative versions of these solutions satisfy the continuous model equations, but they are not stable and thus cannot be attained by *ab initio* time-domain calculations. Another problem is the great sensitivity to the guessed playing frequency.

As a consequence, a certain expertise is needed in order to use the method, but, thanks to an automatic continuation procedure, the calculation is easy. We note that also experimental results can be used for the impedance of the resonator.

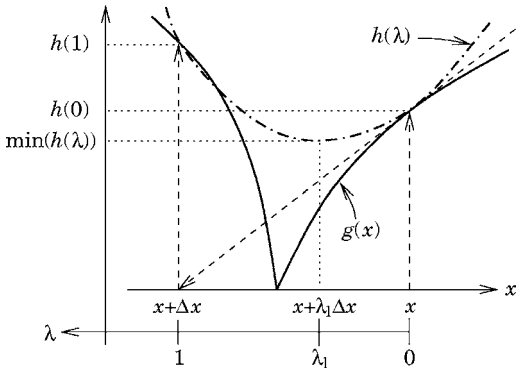

FIG. 13. Principle of backtracking in one dimension. The objective is to estimate the root of $g(x)$ (solid curve). Broken lines with arrows show how the Newton step Δx from x leads to divergence. $h(\lambda)$ (dot-dashed curve) is a second-order expansion of $g(x)$ along the Newton step, i.e., the λ axis. Minimum of $h(\lambda)$ should be closer to the root of $g(x)$ than $g(x+\Delta x)$.

ACKNOWLEDGMENTS

The European Union through the MOSART project is acknowledged for financial support. We would also like to thank Claudia Fritz at IRCAM in Paris for thorough testing and valuable feedback, Joël Gilbert at Laboratoire d'Acoustique de l'Université du Maine (LAUM) in Le Mans, and Philippe Guillemain at the Laboratoire de Mécanique et d'Acoustique at CNRS in Marseille for fruitful discussions during the work, and the latter also for kindly providing some MATLAB code for the time-domain model.

APPENDIX: BACKTRACKING SUMMARY

The principle of the backtracking algorithm[12] is illustrated in one dimension in Fig. 13, where $g(x)$ replaces $|\mathbf{G}(\mathbf{X},f)|$, although we use the multidimensional notation in the following. Defining the λ axis along the Newton step, we simply take a step $\lambda\Delta\mathbf{X}$ in this direction with λ between 0 and 1. The optimal value for λ is the one that minimizes the function $h(\lambda)$

$$h(\lambda) = \tfrac{1}{2}|\mathbf{G}(\mathbf{X}^i + \lambda\Delta\mathbf{X})|^2 \tag{A1}$$

with derivative

$$h'(\lambda) = (\mathbf{J}_G \cdot \mathbf{G})|_{\mathbf{X}^i+\lambda\Delta\mathbf{X}} \cdot \Delta\mathbf{X}. \tag{A2}$$

During the calculation of the failing Newton step, we computed $\mathbf{G}(\mathbf{X}^i)$ and $\mathbf{G}(\mathbf{X}^{i+1})$, so now it is possible to calculate with nearly no additional computational effort $h(0) = \frac{1}{2}|\mathbf{G}(\mathbf{X}^i)|^2$, $h'(0) = -|\mathbf{G}(\mathbf{X}^i)|^2$, and $h(1) = \frac{1}{2}|\mathbf{G}(\mathbf{X}^i+\Delta\mathbf{X})|^2 = \frac{1}{2}|\mathbf{G}(\mathbf{X}^{i+1})|^2$. This allows us to propose a quadratic approximation of h for λ between 0 and 1, for which the minimum is located at

$$\lambda_1 = -\frac{\frac{1}{2}h'(0)}{h(1) - h(0) - h'(0)}. \tag{A3}$$

It can be shown that λ_1 should not exceed 0.5, and in practice $\lambda_1 \geqslant 0.1$ is required to avoid too short a step at this stage.

If $|\mathbf{G}(\mathbf{X}^i+\lambda_1\Delta\mathbf{X})|$ still is larger than $|\mathbf{G}(\mathbf{X}^i)|$, $h(\lambda)$ is then modeled as a cubic function [using $h(\lambda_1)$ which has just been calculated]. The minimum of this cubic function gives a new value λ_2, again restricted to $0.1\lambda_1 < \lambda_2 < 0.5\lambda_1$. This calculation requires solving a system of two equations, so if λ_2 also is not accepted because $|\mathbf{G}(\mathbf{X}^i+\lambda_2\Delta\mathbf{X})|$ is still too large, we do not enhance to a fourth-order model of h, which would increase the computational cost much more. Instead, subsequent cubic modelings are performed using the two most recent values of λ. In practice, however, not many repetitions should be necessary before finding a better solution, if possible.

[1] H. L. F. Helmholtz, *On the Sensations of Tone* (Dover, New York, 1954), English translation of 4th German edition from 1877.

[2] M. E. McIntyre, R. T. Schumacher, and J. Woodhouse, "On the oscillations of musical instruments," J. Acoust. Soc. Am. **74**, 1325–1345 (1983).

[3] N. M. Krylov and N. N. Bogoliubov, *Introduction to Nonlinear Mechanics* (Princeton University Press, Princeton, NJ, 1947), English translation of Russian edition from 1936.

[4] M. Urabe, "Galerkin's procedure for nonlinear periodic systems," Arch. Ration. Mech. Anal. **20**, 120–152 (1965).

[5] A. Stokes, "On the approximation of nonlinear oscillations," J. Diff. Eqns. **12**, 535–558 (1972).

[6] M. S. Nakhla and J. Vlach, "A piecewise harmonic balance technique for determination of periodic response of nonlinear systems," IEEE Trans. Circuit Theory **23**(2), 85–91 (1976).

[7] R. T. Schumacher, "Self-sustained oscillation of the clarinet: An integral equation approach," Acustica **40**, 298–309 (1978).

[8] J. Gilbert, J. Kergomard, and E. Ngoya, "Calculation of the steady-state oscillations of a clarinet using the harmonic balance technique," J. Acoust. Soc. Am. **86**(1), 35–41 (1989).

[9] J. Kergomard, S. Ollivier, and J. Gilbert, "Calculation of the spectrum of self-sustained oscillators using a variable truncation method: Application to cylindrical reed instruments," Acta Acust. Acust. **86**(4), 685–703 (2000).

[10] C. Fritz, S. Farner, and J. Kergomard, "Some aspects of the harmonic balance method applied to the clarinet," Appl. Acoust. **65**(12), 1155–1180 (2004).

[11] S. Farner, HARMBAL, Computer program in C. Available on the Internet at http://www.lma.cnrs-mrs.fr/logiciels/harmbal/.

[12] W. H. Press, S. A. Teukolsky, W. T. Vetterling, and B. P. Flannery, *Numerical Recipes in C: The Art of Scientific Computing*, 2nd ed. (Cambridge University Press, United Kingdom, 1992).

[13] W. E. Worman, "Self-sustained nonlinear oscillations of medium amplitude in clarinet-like systems," Ph.D. thesis, Case Western Reserve University, 1971, Ann Arbor University Microfilms(ref. 71-22869).

[14] J. Kergomard, "Elementary considerations on reed-instruments oscillations," in *Mechanics of Musical Instruments*, Lecture notes CISM, edited by A. Hirschberg, J. Kergomard, and G. Weinreich (Springer, Vienna, 1995), Chap. 6, pp. 229–290.

[15] J.-P. Dalmont, J. Gilbert, and S. Ollivier, "Nonlinear characteristics of single-reed instruments: Quasistatic volume flow and reed opening measurements," J. Acoust. Soc. Am. **114**, 2253–2262 (2003).

[16] N. Grand, J. Gilbert, and F. Laloë, "Oscillation threshold of woodwind instruments," Acta Acust. Acust. **83**(1), 137–151 (1997).

[17] J.-P. Dalmont, J. Gilbert, and J. Kergomard, "Reed instruments, from small to large amplitude periodic oscillations and the helmholtz motion analogy," Acta Acust. Acust. **86**, 671–684 (2000).

[18] S. Ollivier, J. Kergomard, and J.-P. Dalmont, "Idealized models of reed woodwinds. II. On the stability of 'two-step' oscillations," Acta. Acust. Acust. **91**(1), 166–179 (2005).

[19] P. Guillemain, J. Kergomard, and T. Voinier, "Real-time synthesis models of wind instruments based on physical models," in Proc. of the Stockholm Music Acoustics Conference (SMAC) (Stockholm, Sweden, 2003), pp. 389–392.